Discrete transparent boundary conditions for the two dimensional Schrödinger equation

Anton Arnold[1], Matthias Ehrhardt[2], Maike Schulte[3], Ivan Sofronov[4]

anton.arnold@tuwien.ac.at, ehrhardt@math.tu-berlin.de, Maike.Schulte@math.uni-muenster.de, sofronov@spp.keldysh.ru

[1] Institut für Analysis und Scientific Computing, Technische Universität Wien, Wiedner Hauptstr. 8, A–1040 Wien, Austria

[2] Institut für Mathematik, Technische Universität Berlin, Str. des 17. Juni 136, D–10623 Berlin, Germany

[3] Institut für Numerische Mathematik, Universität Münster, Einsteinstr. 62, D–48149 Münster, Germany

[4] Keldysh Institute of Applied Mathematics, Russian Academy of Sciences, Miusskaya sq. 4, Moscow, Russia

AMS 2000 Subject Classification: 65M12, 35Q40, 45K05
Key words: two–dimensional Schrödinger equation, transparent boundary conditions, discrete convolution, finite difference schemes

May 31, 2006

Abstract

This paper is concerned with transparent boundary conditions (TBCs) for the time–dependent Schrödinger equation on a circular domain. Discrete TBCs are introduced in the numerical simulations of problems on unbounded domains in order to reduce the computational domain to a finite region in order to make this problem feasible for numerical simulations.

The main focus of this article is on the appropriate discretization of such TBCs for the two–dimensional Schrödinger equation in conjunction with a conservative Crank–Nicolson–type finite difference discretization. The presented discrete TBCs yield an unconditionally stable numerical scheme and are completely reflection–free at the boundary. Furthermore we prove concisely the stability of the recurrence formulas used to obtain the convolution coefficients of the new discrete TBC for a spatially dependent potential.

Acknowledgement

The first two authors were partially supported by the grants ERBFMRXCT-970157 (TMR–Network) from the EU and the DFG under Grant-No. AR 277/3-1. The last three authors were supported by the DFG Research Center Matheon *"Mathematics for key technologies"* in Berlin. The fourth author was partially supported by RFBR-Grant No. 01-01-00520 and by Saarland University.

1 Introduction

Schrödinger equation. Consider a circular geometry that appears e.g. in fiber optics as Fresnel equation. Therefore, the (scaled) transient Schrödinger equation in $\mathbb{R}^2$ reads in polar coordinates (r, θ):

$$i\psi_t = -\frac{1}{2}\Big[\frac{1}{r}(r\psi_r)_r + \frac{1}{r^2}\psi_{\theta\theta}\Big] + V(r,\theta,t)\psi, \quad r > 0,\ 0 < \theta < 2\pi,\ t > 0, \tag{1.1a}$$

$$\psi(r,\theta,0) = \psi^I(r,\theta), \qquad r > 0,\ 0 < \theta < 2\pi, \tag{1.1b}$$

$$\psi(r,0,t) = \psi(r,2\pi,t), \qquad r > 0,\ t > 0, \tag{1.1c}$$

$$\lim_{r\to\infty} \psi(r,\theta,t) = 0, \qquad 0 < \theta < 2\pi,\ t > 0. \tag{1.1d}$$

We assume that the given potential V is constant outside of the *computational domain* $[0,R] \times [0,2\pi]$:

$$V(r,\theta,t) = V_R \equiv \text{const} \quad \text{for } r \geq R,$$

$0 < \theta < 2\pi,\ \ t \geq 0$, and that the initial data has a compact support:

$$\operatorname{supp} \psi^I \subset [0,R) \times [0,2\pi].$$

Discussions of strategies to soften these restrictions could be found in [18, 25, 14].

Equation (1.1a) has also important applications in electromagnetic wave propagation, [19], in optics ("*Fresnel equation*", [24]) and (underwater) acoustics ("*parabolic equation*", [29]) as a paraxial approximation to the wave equation in the frequency domain.

Analytic TBCs. Let us exemplify first *analytic* TBCs that can be derived for the Schrödinger equation on a circular domain. In the following we briefly review the construction of the analytic TBC from [5] and extend it to the case of a nonzero potential. We remark that a more concise derivation can be found in [16].

We consider (1.1a) on the exterior domain $r > R$ and denote by $\hat{\psi} = \hat{\psi}(r, \theta, s)$ the Laplace transform of ψ w.r.t. time:

$$\frac{1}{r}(r\hat{\psi}_r)_r + \frac{1}{r^2}\hat{\psi}_{\theta\theta} + 2i(s + iV_R)\hat{\psi} = 0, \quad r > R, \quad 0 < \theta < 2\pi. \tag{1.2}$$

The function $\hat{\psi}$ is 2π-periodic and assumed to be continuous and thus we use a Fourier series w.r.t. the angle θ:

$$\hat{\psi}(r, \theta, s) = \sum_{m \in \mathbb{Z}} \hat{\psi}^{(m)}(r, s)\, e^{im\theta}, \quad r > R. \tag{1.3}$$

For each mode $m \in \mathbb{Z}$ the *Fourier coefficient* $\hat{\psi}^{(m)}(r, s)$ satisfies the ordinary differential equation

$$\frac{1}{r}(r\hat{\psi}_r^{(m)})_r + \Big(2is - 2V_R - \frac{m^2}{r^2}\Big)\hat{\psi}^{(m)} = 0, \quad r > R. \tag{1.4}$$

This is the Bessel equation for functions of order m. Hence the solution to (1.4) fulfilling the appropriate decay condition for $r \to \infty$ is given in terms of the *m-th order Hankel function of the first kind* $H_m^{(1)}$:

$$\hat{\psi}^{(m)}(r, s) = \alpha_m(s) H_m^{(1)}(\sqrt{2is - 2V_R}\, r), \quad r > R. \tag{1.5}$$

The radial derivative of $\hat{\psi}^{(m)}$ is computed as

$$\begin{aligned} \partial_r \hat{\psi}^{(m)}(r, s) &= \alpha_m(s)\sqrt{2is - 2V_R} H_m^{(1)'}(\sqrt{2is - 2V_R}\, r) \\ &= \sqrt{2is - 2V_R}\, \frac{H_m^{(1)'}(\sqrt{2is - 2V_R}\, r)}{H_m^{(1)}(\sqrt{2is - 2V_R}\, R)}\, \hat{\psi}^{(m)}(R, s), \end{aligned} \tag{1.6}$$

where we have determined the value of the coefficient $\alpha_m(s)$ from (1.5) by setting $r = R$. Finally, the TBC is obtained by computing the series (1.3), using the inverse Laplace transform and setting $r = R$:

$$\partial_{\mathbf{n}} \psi(R, \theta, t) = \\ \frac{1}{2\pi i} \sum_{m \in \mathbb{Z}} \int_{\gamma - i\infty}^{\gamma + i\infty} \sqrt{2is - 2V_R}\, \frac{H_m^{(1)'}(\sqrt{2is - 2V_R}\, R)}{H_m^{(1)}(\sqrt{2is - 2V_R}\, R)}\, \hat{\psi}^{(m)}(R, s) e^{st}\, ds\, e^{im\theta}, \tag{1.7}$$

where $\mathbf{n}$ denotes the outwardly directed unit normal vector to the disc with radius R and γ is a vertical contour in the complex plane chosen such that all singularities of the integrand are to the left of it.

The TBC (1.7) is non–local both in time and in space. A strategy to derive a spatially localized version of (1.7) by an asymptotic expansion of the Hankel functions and their derivatives according to s can be found in [5].

Due to the nonlocality of the TBC (1.7), its numerical implementation requires to store the boundary data $\hat{\psi}^{(m)}(R,.)$ of all the past history and for all modes $m \in \mathbb{Z}$. Moreover, the discretization of the TBC (1.7), even in one space dimension, is not trivial at all and has attracted lots of attention. For the many proposed strategies of discretizations of the TBC (1.7) in 1D (as well as semi–discrete approaches), we refer the reader to [3, 4, 10, 11, 21, 23, 24] and references therein. We remark also that inadequate discretizations may introduce strong numerical reflections at the boundary or render the discrete initial boundary value problem only conditionally stable, see [14] for a detailed discussion.

Difference equations. We consider a Crank–Nicolson finite difference scheme, which is one of the commonly used discretization methods for the Schrödinger equation. With the *possibly nonuniform radial grid* $\{r_j, j \in \mathbb{N}_0\}$ with $r_{j+1} > r_j > 0$, the uniform azimuthal grid points $\theta_k = k\Delta\theta$ (where $K\Delta\theta = 2\pi$ and the artificial boundary at $r = R$ is located between the grid points with indices $j = J-1$ and J), $t_n = n\Delta t$, the approximation $\psi_{j,k}^{(n)} \sim \psi(r_j, \theta_k, t_n)$, $j = -1, 0, 1, \ldots, J$, $0 \le k < K$, $n \in \mathbb{N}_0$, and the abbreviation $\psi_{j,k}^{(n+1/2)} := \bigl(\psi_{j,k}^{(n+1)} + \psi_{j,k}^{(n)}\bigr)/2$ this scheme reads:

$$
\begin{aligned}
-\frac{2i}{\Delta t}&(\psi_{j,k}^{(n+1)} - \psi_{j,k}^{(n)}) \\
&= \frac{1}{r_j}\frac{1}{\Delta r_j}\Bigl[\frac{r_{j+1/2}(\psi_{j+1,k}^{(n+1/2)} - \psi_{j,k}^{(n+1/2)})}{\Delta r_{j+1/2}} - \frac{r_{j-1/2}(\psi_{j,k}^{(n+1/2)} - \psi_{j-1,k}^{(n+1/2)})}{\Delta r_{j-1/2}}\Bigr] \\
&\quad + \frac{1}{r_j^2}\frac{\psi_{j,k+1}^{(n+1/2)} - 2\psi_{j,k}^{(n+1/2)} + \psi_{j,k-1}^{(n+1/2)}}{\Delta\theta^2} - 2V_{j,k}^{(n+1/2)}\psi_{j,k}^{(n+1/2)},
\end{aligned}
\tag{1.8}
$$

$j \in \mathbb{N}_0$, $0 \le k \le K-1$, $n \ge 0$, with the index k considered as $k \mod K$. The potential term is given by

$$V_{j,k}^{(n+1/2)} = V(r_j, \theta_k, t_{n+1/2}).$$

In (1.8) we have introduced the notation $r_{j+1/2} := (r_{j+1} + r_j)/2$, $j \in \mathbb{N}_0$ amd the abbreviation $\Delta r_{j+1/2} = r_{j+1} - r_j$, $j \in \frac{1}{2} + \mathbb{N}_0$. Note that for consistency we shall assume that Δr_j is a smoothly varying function (for $\Delta r_j \to 0$).

Remark (Treatment of singularity at the origin). It is apparent that (1.1a) has a singularity at $r = 0$. However, this singularity is only due to the representation of the Schrödinger equation in polar coordinates. As a standard numerical strategy we used a radial *offset grid* r_j. At $j = 0$ we have $r_{-1/2} = 0$ and therefore the coefficient of the (auxiliary) value $\psi_{-1,k}^{(n+1/2)}$ is zero, i.e. the scheme (1.8) does not need any extrapolation or special treatment for $\psi_{-1,k}^{(n+1/2)}$. Here, r_j is not necessaily an equidistant grid; only the property $r_{-1/2} = 0$ must be ensured.

2 The Discrete TBC

Transparent boundary conditions (TBCs) are obtained by explicit solution of the equation in the exterior domain $r \geq R$. Now we want to use this strategy to derive a TBC directly for the numerical scheme (1.8), i.e. on a purely discrete level. In other words we construct the discrete Dirichlet-to-Neumann map to eliminate the exterior problem.

Reduction to 1D–Problem. In order to reduce the problem to the simpler 1D case, the discrete Fourier method is used in θ–direction. Due to the *periodic BCs* we have

$$\psi_{j,0}^{(n)} = \psi_{j,K}^{(n)}, \quad j \in \mathbb{N}_0,\, n \geq 0, \tag{2.9}$$

(and $\psi_{0,k}^{(n)} = \psi_{0,0}^{(n)}$, $\forall k$) and hence, use the *discrete Fourier transform* of $\psi_{j,k}^{(n)}$ in θ–direction:

$$\psi_j^{(m,n)} := \frac{1}{K} \sum_{k=0}^{K-1} \psi_{j,k}^{(n)} \exp\left(\frac{2\pi i k m}{K}\right), \quad m = 0, \dots, K-1. \tag{2.10}$$

The scheme (1.8) in the exterior domain $j \geq J-1$ then transforms into:

$$
\begin{aligned}
&-\frac{2i}{\Delta t}(\psi_j^{(m,n+1)} - \psi_j^{(m,n)}) \\
&= \frac{1}{r_j}\frac{1}{\Delta r_j}\Big[\frac{r_{j+1/2}(\psi_{j+1}^{(m,n+1/2)} - \psi_j^{(m,n+1/2)})}{\Delta r_{j+1/2}} - \frac{r_{j-1/2}(\psi_j^{(m,n+1/2)} - \psi_{j-1}^{(m,n+1/2)})}{\Delta r_{j-1/2}}\Big] \\
&\quad - 2V_j^{(m)}\psi_j^{(m,n+1/2)}, \\
&V_j^{(m)} := V_R + \frac{1-\cos\frac{2\pi m}{K}}{r_j^2\Delta\theta^2}, \qquad 0 \leq m \leq K-1,\ n \geq 0.
\end{aligned}
$$

The modes $\psi^{(m)}$, $m = 0, \ldots, K-1$ are independent of each other in the exterior domain $r \geq R$ since the potential V is constant there. Therefore we can continue our analysis for each fixed mode separately.

Thus, by omitting in the sequel the superscript m in the notation, we will consider in the exterior domain a discrete 1D–Schrödinger equation of the following form:

$$
\begin{aligned}
&-i\frac{2\Delta r_j \Delta r_{j+1/2}}{\Delta t}(\psi_j^{(n+1)} - \psi_j^{(n)}) \\
&= \frac{1}{r_j}\Big[r_{j+1/2}(\psi_{j+1}^{(n+1/2)} - \psi_j^{(n+1/2)}) - r_{j-1/2}\frac{\Delta r_{j+1/2}}{\Delta r_{j-1/2}}(\psi_j^{(n+1/2)} - \psi_{j-1}^{(n+1/2)})\Big] \\
&\quad - 2\Delta r_j \Delta r_{j+1/2} V_j \psi_j^{(n+1/2)}, \quad j \geq J-1,
\end{aligned}
\tag{2.11}
$$

with $V_j = V_R + C/(j+0.5)^2$, $C = (1-\cos\frac{2\pi m}{K})/(\Delta r^2 \Delta\theta^2)$ for an equidistant offset grid. We remark that the radial discretization on the computational interval $[0, R]$ can be nonuniform (*e.g. adaptive in time*) for our subsequent analysis.

Mass conservation property. There are two important advantages of this second order (in Δr and Δt) scheme (2.11): it is unconditionally stable, and it preserves the discrete L^2–norm in time:

Lemma 2.1. *For the scheme* (2.11) *holds:*

$$
\|\psi^{(n)}\|_2^2 := \Delta r_j \sum_{j \in \mathbb{N}_0} |\psi_j^{(n)}|^2 r_j
$$

is a conserved quantity in time.

Proof. This conservation property can be seen by a discrete energy estimate. First we multiply (2.11) by $\bar{\psi}_j^{(n)} r_j$ and its complex conjugate by $\psi_j^{(n+1)} r_j$:

$$
\begin{aligned}
&-\frac{2i}{\Delta t}\big(\psi_j^{(n+1)}\bar{\psi}_j^{(n)} - |\psi_j^{(n)}|^2\big) r_j \\
&\qquad = \bar{\psi}_j^{(n)} D^0\big(r_j D^0 \psi_j^{(n+1/2)}\big) - 2V_j \psi_j^{(n+1/2)} \bar{\psi}_j^{(n)} r_j, \quad j-0,1,\dots,
\end{aligned}
\tag{2.12a}
$$

$$
\begin{aligned}
&\frac{2i}{\Delta t}\big(|\psi_j^{(n+1)}|^2 - \bar{\psi}_j^{(n)}\psi_j^{(n+1)}\big) r_j \\
&\quad = \psi_j^{(n+1)} D^0\big(r_j D^0 \bar{\psi}_j^{(n+1/2)}\big) - 2V_j \bar{\psi}_j^{(n+1/2)} \bar{\psi}_j^{(n+1)} r_j, \quad j-0,1,\dots,
\end{aligned}
\tag{2.12b}
$$

with the abbreviation of the centered difference quotient

$$
D^0 = D^0_{\frac{\Delta r_j}{2}}, \text{ i.e. } D^0\psi_j^n = \frac{\psi_{j+1/2}^n - \psi_{j+1/2}^n}{\Delta r_j}.
$$

Next we subtract (2.12a) from (2.12b)

$$
\begin{aligned}
&\frac{2i}{\Delta t}\big(|\psi_j^{(n+1)}|^2 - |\psi_j^{(n)}|^2\big) r_j \\
&\qquad\qquad = \psi_j^{(n+1)} D^0\big(r_j D^0 \bar{\psi}_j^{(n+1/2)}\big) - \bar{\psi}_j^{(n)} D^0\big(r_j D^0 \psi_j^{(n+1/2)}\big) \\
&\qquad\qquad\quad - V_j\big(|\psi_j^{(n+1)}|^2 - |\psi_j^{(n)}|^2\big) r_j, \quad j-0,1,\dots,
\end{aligned}
$$

sum from $j=0$ to ∞, and apply summation by parts:

$$
\begin{aligned}
&\frac{2i}{\Delta t}\sum_{j=0}^{\infty}\big(|\psi_j^{(n+1)}|^2 - |\psi_j^{(n)}|^2\big) r_j \\
&\quad = -\sum_{\mathbb{N}_0+\frac{1}{2}}^{\infty}\big(D^0\bar{\psi}_j^{(n+1/2)}\big)\big(D^0\psi_j^{(n+1)}\big) r_j - \big(D^0\bar{\psi}_{-\frac{1}{2}}^{(n+1/2)}\big)\psi_0^{(n+1)} r_{-\frac{1}{2}} \\
&\qquad + \sum_{\mathbb{N}_0+\frac{1}{2}}^{\infty}\big(D^0\psi_j^{(n+1/2)}\big)\big(D^0\bar{\psi}_j^{(n)}\big) r_j - \big(\psi_{-\frac{1}{2}}^{(n+1/2)}\big)\bar{\psi}_0^{(n)} r_{-\frac{1}{2}} \\
&\qquad - \sum_{j=0}^{\infty} V_j\big(|\psi_j^{(n+1)}|^2 - |\psi_j^{(n)}|^2\big) r_j,
\end{aligned}
\tag{2.13}
$$

Now, the boundary terms in (2.13) vanish since $r_{-\frac{1}{2}} = 0$ and we can write

$$\begin{aligned}
&\frac{2i}{\Delta t} \sum_{j=0}^{\infty} \big(|\psi_j^{(n+1)}|^2 - |\psi_j^{(n)}|^2\big) r_j \\
&\quad = - \sum_{\mathbb{N}_0+\frac{1}{2}}^{\infty} \big(|D^0 \bar{\psi}_j^{(n+1)}|^2 - D^0 \bar{\psi}_j^{(n)}|^2\big) r_j - \sum_{j=0}^{\infty} V_j \big(|\psi_j^{(n+1)}|^2 - |\psi_j^{(n)}|^2\big) r_j,
\end{aligned} \tag{2.14}$$

Finally, taking imaginary parts one obtains the desired result. □

Discrete TBCs. *Discrete transparent boundary conditions* (DTBCs) for the 1D Schrödinger equation with $V_j = \text{const}$ in the exterior domain were introduced by Arnold in [6]. Here we want to derive a DTBC for a spatially varying potential V_j in the exterior domain $j \geq J-1$ (cf. (2.11)) and obtain the DTBC of Arnold as the limiting case $j \to \infty$.

We use the Z–transform of the sequence $\{\psi_j^{(n)}\}$, $n \in \mathbb{N}_0$ (with j considered fixed) which is defined as the Laurent series, see [13]:

$$\mathcal{Z}\{\psi_j^{(n)}\} = \hat{\psi}_j(z) := \sum_{n=0}^{\infty} \psi_j^{(n)} z^{-n}, \quad z \in \mathbb{C}, \quad |z| > R_{\hat{\psi}_j}, \tag{2.15}$$

and $R_{\hat{\psi}_j}$ denotes the convergence radius of the series. Now the transformed exterior scheme (2.11) reads

$$\begin{aligned}
&- i\rho_j \frac{z-1}{z+1} \hat{\psi}_j(z) \\
&= \frac{1}{r_j} \Big[r_{j+1/2} \big(\hat{\psi}_{j+1}(z) - \hat{\psi}_j(z)\big) - r_{j-1/2} \frac{\Delta r_{j+1/2}}{\Delta r_{j-1/2}} \big(\hat{\psi}_j(z) - \hat{\psi}_{j-1}(z)\big) \Big] \\
&\qquad - 2\Delta r_j \Delta r_{j+1/2} V_j \hat{\psi}_j(z), \quad j \geq J-1,
\end{aligned} \tag{2.16}$$

with the mesh ratio $\rho_j = 4\Delta r_j \Delta r_{j+1/2}/\Delta t$ and $V_j = V_R + C/j^2$. Thus we obtain a homogeneous second order difference equation with varying coefficients of the form

$$a_j \hat{\psi}_{j+1}(z) + b_j(z) \hat{\psi}_j(z) + c_j \hat{\psi}_{j-1}(z) = 0, \quad j \geq J-1, \tag{2.17}$$

with

$$a_j = \frac{r_{j+1/2}}{r_j}, \tag{2.18a}$$

$$b_j(z) = -\frac{1}{r_j}\Big[r_{j+1/2} + r_{j-1/2}\frac{\Delta r_{j+1/2}}{\Delta r_{j-1/2}}\Big] + i\rho_j\,\frac{z-1}{z+1} - 2\Delta r_j \Delta r_{j+1/2} V_j, \tag{2.18b}$$

$$c_j = \frac{r_{j-1/2}}{r_j}\frac{\Delta r_{j+1/2}}{\Delta r_{j-1/2}}. \tag{2.18c}$$

Remark (uniform offset grid). In the special case of a uniform radial offset grid $r_j = (j+\frac{1}{2})\Delta r$, $j \geq J-1$, we obtain

$$a_j = \frac{j+1}{j+\frac{1}{2}}, \quad j \geq J-1, \tag{2.19a}$$

$$b_j(z) = -2 + i\rho\,\frac{z-1}{z+1} - 2\Delta r^2 V_R - 2\frac{1-\cos\frac{2\pi m}{K}}{(j+1/2)\Delta\theta^2}, \quad j \geq J-1, \tag{2.19b}$$

$$c_j = \frac{j}{j+\frac{1}{2}}, \quad j \geq J-1. \tag{2.19c}$$

For the formulation of the Z–transformed DTBC at $j = J$ we regard the ratio $\hat{\ell}_j(z)$ of the solutions at two adjacent points:

$$\hat{\ell}_j(z) = \frac{\hat{\psi}_j(z)}{\hat{\psi}_{j-1}(z)}, \quad j \geq J, \tag{2.20}$$

and get from (2.17) the equation

$$\hat{\ell}_j(z)\Big(a_j(z)\hat{\ell}_{j+1}(z) + b_j(z)\Big) + c_j = 0, \quad j \geq J. \tag{2.21}$$

In order to find a solution to (2.21) we use the method of series. Let us consider the Laurent series for $\hat{\ell}_j(z)$:

$$\hat{\ell}_j(z) = \ell_j^{(0)} + \ell_j^{(1)} z^{-1} + \cdots + \ell_j^{(n)} z^{-n} + \ldots, \quad |z| \geq 1. \tag{2.22}$$

Define the auxiliary functions

$$\begin{aligned} \alpha_j(z) &:= \frac{b_j(z)}{a_j}, \\ \alpha_j &:= \lim_{z\to\infty} \alpha_j(z), \\ \beta_j &:= \frac{c_j}{a_j}, \\ \gamma_j &= \alpha_j - \bar{\alpha}_j. \end{aligned} \tag{2.23}$$

Then (2.21) reads

$$\hat{\ell}_j(z)\Big(\hat{\ell}_{j+1}(z) + \alpha_j(z)\Big) + \beta_j = 0, \quad j \geq J. \tag{2.24}$$

Substituting (2.22) for (2.24) we get

$$\begin{aligned}&\big(\ell_j^{(0)} + \ell_j^{(1)} z^{-1} + \dots + \ell_j^{(n)} z^{-n} + \dots\big)\cdot \\ &\qquad \cdot \Big(\big(\ell_{j+1}^{(0)} + \ell_{j+1}^{(1)} z^{-1} + \dots + \ell_{j+1}^{(n)} z^{-n} + \dots\big) + \alpha_j(z)\Big) + \beta_j = 0.\end{aligned} \tag{2.25}$$

Taking $|z| \to \infty$ we have the following recurrence equation for $\ell_j^{(0)}$:

$$\ell_j^{(0)}\big(\ell_{j+1}^{(0)} + \alpha_j\big) + \beta_j = 0. \tag{2.26}$$

We shall solve this equation starting from an index J_∞ to $j = J$, i.e. putting a boundary value $\ell_{J_\infty}^{(0)} := \ell_\infty^{(0)}$ and running the recursion from J_∞ to J:

$$\ell_j^{(0)} = \frac{-\beta_j}{\ell_{j+1}^{(0)} + \alpha_j}, \quad j = J_\infty - 1, J_\infty - 2, \dots, J. \tag{2.27}$$

Note that a very large index J corresponds to a very large radius r_{J_∞}; therefore we can use the 1D plane case coefficient $\ell^{(0)}$, see [9], as the value $\ell_\infty^{(0)}$.

The stability of the recurrence relations.

Theorem 2.1. *Let* $|\alpha_j| \geq 2 > \beta_j + 1$. *Then:*

a) $|\ell_j^{(0)}| < \beta_j < 1$*; and*

b) the recurrence formulas (2.27) *are stable with respect to small perturbations.*

Proof. The item a) is proved by induction. Suppose $|\ell_{j+1}^{(0)}| < \beta_{j+1}$. Hence

$$|\ell_{j+1}^{(0)} + \alpha_j| - \beta_j \geq |\alpha_j| - |\ell_{j+1}^{(0)}| - \beta_j > 1 - |\ell_{j+1}^{(0)}| > 0.$$

Therefore $|\ell_j^{(0)}| < 1$. Furthermore we have:

$$|\ell_j^{(0)}| = \frac{\beta_j}{|\ell_{j+1}^{(0)} + \alpha_j|} < \frac{\beta_j}{2 - |\ell_{j+1}^{(0)}|} < \beta_j. \tag{2.28}$$

To prove b) and establish the stability we suppose that we have a perturbation $\ell_{j+1}^{(0)} + \delta_{j+1}$ instead of $\ell_{j+1}^{(0)}$ with $|\delta_{j+1}| < 1$. Let us look at the evolution of δ_j by comparing (2.27) with

$$\ell_j^{(0)} + \delta_j = \frac{-\beta_j}{\ell_{j+1}^{(0)} + \delta_{j+1} + \alpha_j}, \quad j = J_\infty - 1, J_\infty - 2, \ldots, J.$$

Evidently we obtain:

$$\begin{aligned}\delta_j &= \frac{-\beta_j}{\ell_{j+1}^{(0)} + \delta_{j+1} + \alpha_j} - \frac{-\beta_j}{\ell_{j+1}^{(0)} + \alpha_j} = \delta_{j+1} \frac{-\ell_j^{(0)}}{\ell_{j+1}^{(0)} + \delta_{j+1} + \alpha_j} \\ &= \delta_{j+1} \frac{-\ell_j^{(0)}}{-\beta_j/\ell_j^{(0)} + \delta_{j+1}}.\end{aligned}$$

Therefore we get

$$|\delta_j| = |\delta_{j+1}| \frac{|\ell_j^{(0)}|}{|\beta_j/\ell_j^{(0)} + \delta_{j+1}|} < |\delta_{j+1}| \frac{|\ell_j^{(0)}|^2}{\beta_j - |\ell_j^{(0)}||\delta_{j+1}|} < |\delta_{j+1}| \frac{|\ell_j^{(0)}|^2}{\beta_j} \frac{1}{1 - |\delta_{j+1}|},$$

and hence

$$\frac{|\delta_j|}{|\delta_{j+1}|} \sim \frac{|\ell_j^{(0)}|^2}{\beta_j} < \beta_j < 1, \tag{2.29}$$

for $|\delta_{j+1}| < 1$. Thus the recursion (2.27) is stable with respect to small perturbations (e.g. for truncation errors or for an "incorrect" initial guess $\ell_{J_\infty}^{(0)} := \ell_\infty^{(0)}$). □

Remark. The theorem condition $|\alpha_j| \geq 2 > \beta_j + 1$ is valid for definitions (2.18).

Remark. The estimate (2.29) permits to explain a fast convergence of the recursion (2.27) to the correct value $\ell_J^{(0)}$ while taking an "incorrect" initial guess $\ell_{J_\infty}^{(0)} := \ell_\infty^{(0)}$, see the numerical examples in Section 3. Indeed due to (2.29) we can hope for the exponential decay of $|\delta_j|$ with the factor $|\ell_j^{(0)}|^2/\beta_j \sim |\ell_j^{(0)}|$. For instance the value $|\ell_j^{(0)}|$ is estimated from the case of the "frozen" coefficients at J_∞:

$$|\ell_j^{(0)}| \sim |\ell_\infty^{(0)}|,$$

where $|\ell_\infty^{(0)}| < 1$ is the root of the square equation

$$\ell_\infty^{(0)} = \frac{-\beta_{J_\infty}}{\ell_\infty^{(0)} + \alpha_{J_\infty}}.$$

Now we consider the calculation of $\ell_j^{(1)}$. We have from (2.18):

$$\alpha_j(z) := \alpha_j - \gamma_j(z^{-1} - z^{-2} + z^{-3} - \dots), \tag{2.30}$$

where γ_j is defined in (2.23). From (2.25) and (2.30) we can write

$$\begin{aligned} &\big(\ell_j^{(0)} + \ell_j^{(1)} z^{-1} + \mathrm{O}(z^{-2})\big)\cdot \\ &\cdot\Big(\big(\ell_{j+1}^{(0)} + \ell_{j+1}^{(1)} z^{-1} + \mathrm{O}(z^{-2})\big) + \big(\alpha_j - \gamma_j z^{-1} + \mathrm{O}(z^{-2})\big)\Big) + \beta_j = 0. \end{aligned} \tag{2.31}$$

Annihilating leading terms subjected to (2.26) we collect terms with factor z^{-1} and obtain after multiplying by z and considering $|z| \to \infty$:

$$\ell_j^{(0)}\ell_{j+1}^{(1)} - \ell_j^{(0)}\gamma_j + \ell_j^{(1)}\ell_{j+1}^{(0)} + \ell_j^{(1)}\alpha_j = 0. \tag{2.32}$$

Therefore the recursion is defined by

$$\ell_j^{(1)} = -\frac{\ell_j^{(0)}\ell_{j+1}^{(1)} - \ell_j^{(0)}\gamma_j}{\ell_{j+1}^{(0)} + \alpha_j}, \quad j = J_\infty - 1, J_\infty - 2, \dots, J, \tag{2.33}$$

with a boundary value $\ell_{J_\infty}^{(1)} := \ell_\infty^{(1)}$.

The case of $\ell_j^{(n)}$ with $n \geq 2$ is considered similarly by truncating terms of $\mathrm{O}(z^{-n-1})$ in (2.31); we get the following recursion formula:

$$\ell_j^{(n)} = -\frac{\sum\limits_{k=0}^{n-1} \ell_j^{(k)}\ell_{j+1}^{(n-k)} + \gamma_j(-1)^{n-k}\ell_j^{(k)}}{\ell_{j+1}^{(0)} + \alpha_j}, \quad j = J_\infty - 1, J_\infty - 2, \dots, J, \tag{2.34}$$

with a boundary value $\ell_{J_\infty}^{(n)} := \ell_\infty^{(n)}$ that can be taken from the 1D plane case: $\ell_\infty^{(n)} \equiv \ell^{(n)}$. Notice that (2.33) is a particular case of (2.34) at $n = 1$.

Theorem 2.2. *Under conditions of Theorem 2.1* $|\alpha_j| \geq 2 > \beta_j + 1$ *the recurrence formulas* (2.34) *are stable with respect to small perturbations.*

Proof. Let us write (2.34) in the resolution form with respect to index n:

$$\ell_j^{(n)} = \frac{\ell_j^{(0)}}{\ell_{j+1}^{(0)} + \alpha_j} \ell_{j+1}^{(n)} + F\Big(\{\ell_j^{(n_1<n)}\}, \{\ell_{j+1}^{(n_1<n)}\}\Big), \quad j = J_\infty - 1, J_\infty - 2, \ldots, J, \tag{2.35}$$

where the function F contains remaining terms with indexes $n_1 < n$. Suppose that the coefficients $\{\ell_j^{(n_1)}\}$, $n_1 = 0, 1, \ldots, n-1$, $j = J_\infty - 1, J_\infty - 2, \ldots, J$ are exact (or they are known with a good accuracy). Then the stability of (2.34) is, evidently, determined by the magnitude of the multiplier

$$\frac{\ell_j^{(0)}}{\ell_{j+1}^{(0)} + \alpha_j}.$$

We have from (2.28):

$$\frac{|\ell_j^{(0)}|}{|\ell_{j+1}^{(0)} + \alpha_j|} < \frac{\beta_j}{|\ell_{j+1}^{(0)} + \alpha_j|} < \frac{\beta_j}{2 - |\ell_{j+1}^{(0)}|} < \beta_j < 1.$$

□

Remark. The proof of Theorem 2.2 is made by induction with respect to $n = 1, 2, \ldots$ at the assumption that the previous coefficients for $n_1 < n$ are correct. In the practice, while calculating the coefficients $\ell_j^{(n)}$ we must fix some value J_∞ and take an "incorrect" boundary value $\ell_{J_\infty}^{(n)} := \ell_\infty^{(n)}$ This could give a numerical instability. However, due to sufficiently fast convergence of $\ell_j^{(0)}$ to its correct value, say after several first steps J_0 of the recursion (2.27), we can start the recursion run of $\ell_j^{(1)}$ a little bit later, i.e. with the delay: $j = J_\infty - J_0$. Similarly for $\ell_j^{(1)}$ the initial index can be $j = J_\infty - 2J_0$, etc. In our numerical tests the usual value is $J_0 = 2 - 5$, see the numerical examples in Section 3.

Implementation of the DTBC. The DTBC is calculated in Fourier transformed space, for all modes $m = 1, \ldots, K$:

$$\hat{\psi}_{j,m}^n := \frac{1}{K} \sum_{k=1}^{K} e^{\frac{2\pi i (m-1)(k-1)}{K}} \psi_{j,k}^n, \qquad m = 1, \ldots, K. \tag{2.36}$$

From (2.21) we have for $m = 1, \ldots, K$

$$\hat{\ell}_{j,m}(z) = \frac{\hat{\psi}_{j,m}(z)}{\hat{\psi}_{j-1,m}(z)} \tag{2.37}$$

for $j \geq J+1$. Calculating the inverse $\mathcal{Z}$–transformation we get the discrete convolution

$$\hat{\psi}_{j,m}^{(n)} = \hat{\ell}_{j,m}^{(n)} * \hat{\psi}_{j-1,m}^{(n)} \tag{2.38}$$

$$\Rightarrow \qquad \hat{\psi}_{j,m}^{(n)} - \hat{\ell}_{j,m}^{(0)} \hat{\psi}_{j-1,m}^{(n)} = \sum_{p=0}^{n-1} \hat{\ell}_{j,m}^{(n-p)} \hat{\psi}_{j-1,m}^{(p)} \tag{2.39}$$

$$\Rightarrow \qquad \hat{\psi}_{j,m}^{(n)} - \hat{s}_{j,m}^{(0)} \hat{\psi}_{j-1,m}^{(n)} = \sum_{p=0}^{n-1} \hat{s}_{j,m}^{(n-p)} \hat{\psi}_{j-1,m}^{(p)} - \hat{\psi}_{j,m}^{(n-1)}, \tag{2.40}$$

with the summed convolution coefficients given by

$$\begin{aligned} \hat{s}_{j,m}^{(0)} &:= \hat{\ell}_{j,m}^{(0)}, \\ \hat{s}_{j,m}^{(n)} &:= \hat{\ell}_{j,m}^{(n)} + \hat{\ell}_{j,m}^{(n-1)}, \qquad n \geq 1. \end{aligned} \tag{2.41}$$

Hence the *Fourier transformed DTBC* reads

$$\hat{\psi}_{J+2,m}^{(n)} - \hat{s}_{J+2,m}^{(0)} \hat{\psi}_{J+1,m}^{(n)} = \sum_{p=0}^{n-1} \hat{s}_{J+2,m}^{(n-p)} \hat{\psi}_{J+1,m}^{(p)} - \hat{\psi}_{J+2,m}^{(n-1)}, \tag{2.42}$$

for $m = 1, \ldots, K$. The discrete convolution $\sum \hat{s}_{J+2,m}^{(n-p)} \hat{\psi}_{J+1,m}^{(p)}$ is calculated in Fourier space and transformed back by

$$\mathrm{ConvSum}_{J+1,k}^{n-1} := \sum_{m=1}^{K} e^{\frac{-2\pi i (m-1)(k-1)}{K}} \Big(\sum_{p=0}^{n-1} \hat{s}_{J+2,m}^{(n-p)} \hat{\psi}_{J+1,m}^{(p)} \Big), \quad k = 1, \ldots, K$$

The part $\hat{s}_{J+2,m}^{(0)} \hat{\psi}_{J+1,m}^{(n)}$ of the left hand side of (2.42) has to be transformed back into physical space and we get the couplings

$$\begin{aligned} \Big(\hat{s}_{J+2,m}^{(0)} \hat{\psi}_{J+1,m}^{(n)} \Big)^{\vee}_{J+1,k,l} &= \sum_{m=1}^{K} \hat{s}_{J+2,m}^{(0)} \hat{\psi}_{J+1,m}^{(n)} e^{\frac{-2\pi i (m-1)(k-1)}{K}} \\ &= \frac{1}{K} \sum_{m=1}^{K} \sum_{l=1}^{K} \hat{s}_{J+2,m}^{(0)} e^{\frac{-2\pi i (m-1)(k-1)}{K}} e^{\frac{2\pi i (k-1)(l-1)}{K}} \psi_{J+1,l}^{(n)}, \end{aligned} \tag{2.43}$$

for $k,l=1,\dots,K$. Hence the implemented DTBC reads

$$\psi_{J+1,k}^{(n)}-\frac{1}{K}\sum_{m=1}^{K}\sum_{l=1}^{K}\hat{s}_{J+2,m}^{(0)}\,e^{\frac{-2\pi i(m-1)(k-1)}{K}}e^{\frac{2\pi i(k-1)(l-1)}{K}}\psi_{J+1,l}^{(n)}$$
$$=\mathrm{ConvSum}_{J+1,k}^{n-1}-\psi_{J+1,k}^{(n-1)}. \quad (2.44)$$

In order to formulate the DTBC as in (2.20) it is necessary that the discrete initial condition vanishes at the two adjacent (spatial) grid points appearing in (2.20). Here, we chose to formulate the DTBC at the boundary of the computational interval and one grid point in the *interior*. Hence we have assumed that the initial condition satisfies $\psi_{J-1}^{(0)}=\psi_{J}^{(0)}=0$. However, with only minor changes to our subsequent analysis one could also prescribe the DTBC at $j=J,\ J+1$.

The use of the formulas (2.44) for calculations permits us to avoid any boundary reflections and it renders the fully discrete scheme unconditionally stable (just like the underlying Crank–Nicolson scheme). Note that we need to evaluate for each mode m just one convolution of (2.44) at each time step (at the endpoint of the interval $[0,t_n]$). Since the other points of this convolution are not needed, using an FFT is not practical.

3 Numerical Examples

Example 1

We start with recalling Example 1 from [16], i.e. we consider (1.1) with the potential

$$V(r,\theta,t)=\begin{cases}\sin(2\pi r), & r\in[0,1],\\ 0, & \text{otherwise},\end{cases} \quad (3.1)$$

and the initial data

$$\psi^{I}(r,\theta)=\begin{cases}1+\cos(\pi r)+i\big(\cos(2\pi r)-1\big), & r\in[0,1],\\ 0, & \text{otherwise},\end{cases} \quad (3.2)$$

which are both independent of the angle θ. Consequently, the solution will only dependent on r and t. For this initial function and this potential we present in Figure 1 the solution of (1.8) with the discretization parameters $\Delta t = 2 \cdot 10^{-4}$, $\Delta r = 0.02$. Since we use the offset grid, the DTBC is given at $r = 1.01$, between $r = 1$ and $r = 1 + \Delta r$. In order to obtain the error of the DTBC, we furthermore compare the calculated solution ψ on the interval $[0, 1.01]$ with a (apparently more exact) reference solution ψ_2 calculated on $[0, 2.01]$ with DTBC at $r = 2.02$. Figure 2 shows the relative error

$$L(t) = \frac{||\psi(.,.,t) - \psi_2(.,.,t)||_{l^2(\Omega)}}{||\psi^I(.,.)||_{l^2(\Omega)}} \tag{3.3}$$

for the same discretization parameters used before.

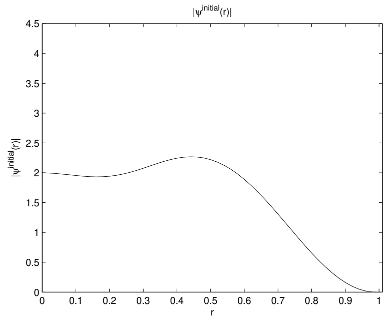

(a) initial function

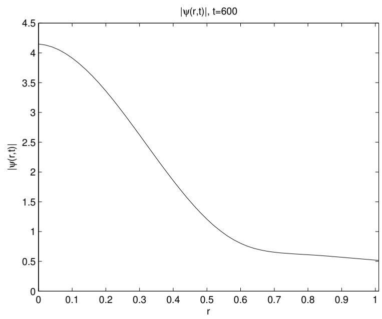

(b) $T = 600\Delta t = 0.12$

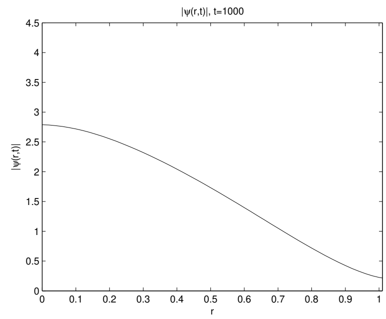

(c) $T = 1000\Delta t = 0.2$

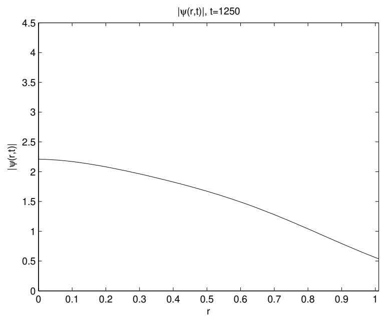

(d) $T = 1250\Delta t = 0.25$

Figure 1: Absolute value of the calculated discrete solution of the time-dependent Schrödinger equation (1.8) with the initial function (3.2) on the computational domain $[0, 1.01]$ with $\Delta r = 0.02$, $\Delta t = 2 \cdot 10^{-4}$ and the potential as given in (3.1); the DTBC is implemented at $r = 1.01$.

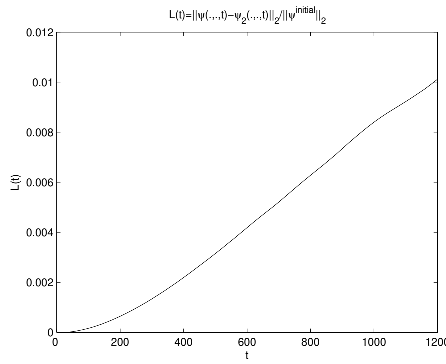

Figure 2: Relative error $L(t)$ of the DTBC for the time evolution of initial function (3.2). We have taken the same discretization parameters as in Figure 1.

Example 2

We recall the Example 2 from [16], i.e. we consider (1.1) with the vanishing potential $V \equiv 0$ and the angle–dependent initial data

$$\psi^I(r,\theta) = \frac{e^{2ik_x r\cos\theta + 2ik_y r\sin\theta - \frac{(r\cos\theta)^2}{2\alpha_x} - \frac{(r\sin\theta)^2}{2\alpha_y}}}{\sqrt{\alpha_x\alpha_y}}, \tag{3.4}$$

with a cutoff at $r = 1.5$. Then the exact solution to (1.1) is given by the Gaussian beam

$$\psi(r,\theta,t) = \frac{e^{2ik_x(r\cos\theta - k_x t) + 2ik_y(r\sin\theta - k_y t) - \frac{(r\cos\theta - 2k_x t)^2}{2(\alpha_x + it)} - \frac{(r\sin\theta - 2k_y t)^2}{2(\alpha_y + it)}}}{\sqrt{\alpha_x + it}\sqrt{\alpha_y + it}}. \tag{3.5}$$

We set $\alpha_x = \alpha_y = 0.04$ and let $k_x = -10$, $k_y = 0$. Since the exact solution (3.5) is known, we calculate the solution on the annulus $\Omega := [0.375, 1.5] \times [0, 2\pi]$ with DTBC at $r = 1.5$ and Dirichlet boundary conditions at $r = 0.375$. For the discretization parameters we choose $\Delta r = 0.025$, $\Delta\theta = 2\pi/50$, $\Delta t = 2 \cdot 10^{-4}$. We present in Figure 3 the initial function (3.4) on the disc $[0, 1.5] \times [0, 2\pi]$ and the evolution of the calculated solution ψ on the annulus Ω after 300, 400 and 600 time steps. Like we have done in Example 1, we compare the calculated solution ψ on Ω with a reference solution ψ_2 calculated on $[0.375, 3] \times [0, 2\pi]$ with DTBC $r = 3$. Figure 4 shows the relative error (3.3) for the same discretization parameters as before.

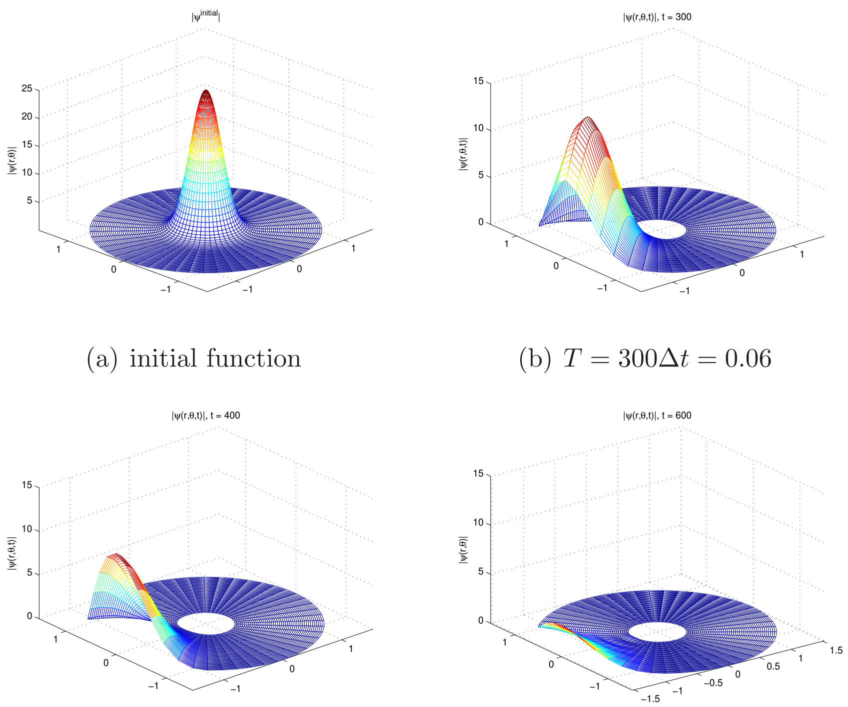

(a) initial function

(b) $T = 300\Delta t = 0.06$

(c) $T = 400\Delta t = 0.08$

(d) $T = 600\Delta t = 0.12$

Figure 3: Absolute value of the calculated solution ψ of (1.8) with the initial function (3.4) on the computational domain $[0.375, 1.5] \times [0, 2\pi]$ with $\Delta r = 0.025$, $\Delta\theta = 2\pi/50$, $\Delta t = 2 \cdot 10^{-4}$ and the wavenumbers $k_x = -10$, $k_y = 0$. The potential equals 0; DTBC are implemented at $r = 1.5$.

Example 3

We recall the numerical example from [5] and consider (1.1) with the vanishing potential $V \equiv 0$ and the initial data

$$\psi^I(r,\theta) = e^{ik_x r\cos\theta - \frac{\alpha}{2}r^2} \tag{3.6}$$

with $k_x = -5$. The exact solution of (1.1) is a time Gaussian distribution

$$\psi(r,\theta,t) = \frac{1}{\sqrt{1+i\alpha t}} \exp\Big(\frac{-\alpha r^2 + 2ik_x r\cos\theta - k_x^2 it}{2+2i\alpha t}\Big). \tag{3.7}$$

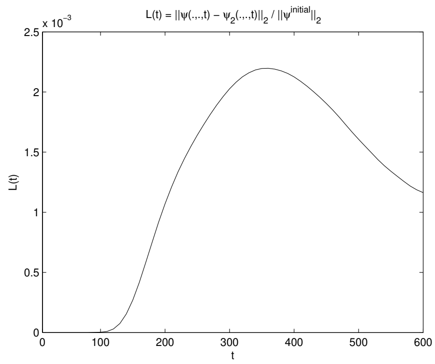

Figure 4: Relative error $L(t)$ of the DTBC for the time evolution of initial function (3.4). We have taken the same discretization parameters as in Figure 3.

Again we calculate a solution ψ of (1.8) on an annulus $\Omega := [0.3571, 1] \times [0, 2\pi]$ and compare it with a reference solution ψ_2 calculated on $[0.3571, 2] \times [0, 2\pi]$. Figure 5 shows the absolute value of the initial function on the disc $[0, 1] \times [0, 2\pi]$ and absolute value of solution ψ for the time steps 100, 200, 400. For this plots we have used the discretization parameters $\Delta r = 1/70$, $\Delta\theta = 70/2\pi$, $\Delta t = 4 \cdot 10^{-4}$, $k_x = -15$, $\alpha = 25$. Again the DTBC is implemented at the outer boundary of the annulus, here at $r = 1$, and Dirichlet boundary conditions at the inner boundary at $r = 0.3571$. In Figure 6 we plotted the relative error $L(t)$ given in (3.3) of ψ and ψ_2.

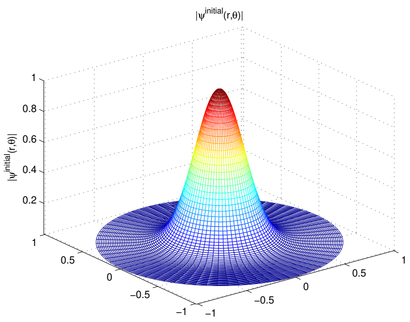

(a) initial function

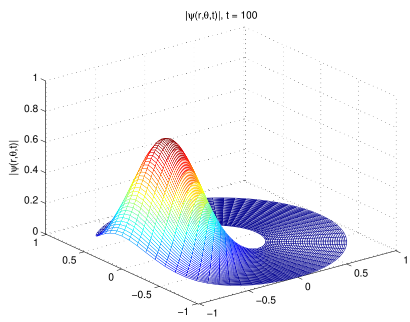

(b) $T = 100\Delta t = 0.04$

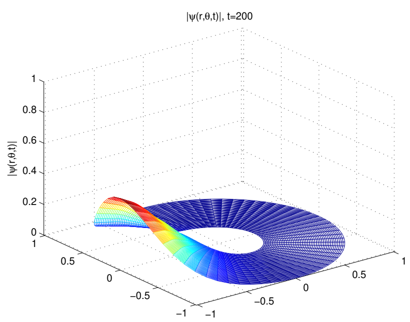

(c) $T = 200\Delta t = 0.08$

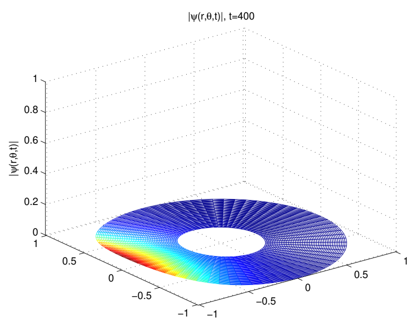

(d) $T = 400\Delta t = 0.16$

Figure 5: Absolute value of the calculated solution ψ of (1.8) with the initial function (3.6) on the computational domain $[0.3571, 1] \times [0, 2\pi]$ with $\Delta r = 1/70$, $\Delta\theta = 2\pi/70$, $\Delta t = 4 \cdot 10^{-4}\, \alpha = 25$ and the wavenumber $k_x = -15$. The potential equals 0; the DTBC is implemented at $r = 1$.

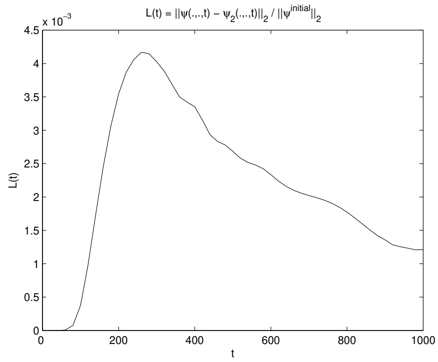

Figure 6: Relative error $L(t)$ of the DTBC for the time evolution of initial function (3.4). We have taken the same discretization parameters as in Figure 5.

References

[1] B. Alpert, L. Greengard and T. Hagstrom, *Rapid evaluation of nonreflecting boundary kernels for time–domain wave propagation*, SIAM J. Numer. Anal. **37** (2000), 1138–1164.

[2] B. Alpert, L. Greengard and T. Hagstrom, *Nonreflecting Boundary Conditions for the Time–Dependent Wave Equation*, J. Comp. Phys. **180** (2002), 270–296.

[3] I. Alonso–Mallo and N. Reguera, *Weak ill-posedness of spatial discretizations of absorbing boundary conditions for Schrödinger–type equations*, SIAM J. Numer. Anal. **40** (2002), 134–158.

[4] X. Antoine and C. Besse, *Unconditionally stable discretization schemes of non–reflecting boundary conditions for the one–dimensional Schrödinger equation*, J. Comp. Phys. **188** (2003), 157–175.

[5] X. Antoine, C. Besse and V. Mouysset, *Numerical Schemes for the simulation of the two–dimensional Schrödinger equation using non–reflecting boundary conditions*, Preprint 2003, published: Math. Comp. **73** (2004), 1779–1799.

[6] A. Arnold, *Numerically Absorbing Boundary Conditions for Quantum Evolution Equations*, VLSI Design **6** (1998), 313–319.

[7] A. Arnold and M. Ehrhardt, *Discrete transparent boundary conditions for wide angle parabolic equations in underwater acoustics*, J. Comp. Phys. **145** (1998), 611–638.

[8] A. Arnold, *Mathematical concepts of open quantum boundary conditions*, Transp. Theory Stat. Phys. **30**, 4–6 (2001), 561–584.

[9] A. Arnold, M. Ehrhardt and I. Sofronov, *Discrete transparent boundary conditions for the Schrödinger equation: Fast calculation, approximation, and stability*, Comm. Math. Sci. **1** (2003), 501–556

[10] V.A. Baskakov and A.V. Popov, *Implementation of transparent boundaries for numerical solution of the Schrödinger equation*, Wave Motion **14** (1991), 123–128.

[11] C.H. Bruneau and L. Di Menza, *Conditions aux limites transparentes et artificielles pour l'équation de Schrödinger en dimension 1 d'espace*, C. R. Acad. Sci. Paris, Ser. I **320** (1995), 89–94.

[12] A. Dedner, D. Kröner, I. Sofronov and M. Wesenberg, *Transparent Boundary Conditions for MHD Simulations in Stratified Atmospheres*, J. Comp. Phys. **171** (2001), 448–478.

[13] G. Doetsch, *Anleitung zum praktischen Gebrauch der Laplace–Transformation und der Z–Transformation*, R. Oldenburg Verlag München, Wien, 3. Auflage 1967.

[14] M. Ehrhardt and A. Arnold, *Discrete Transparent Boundary Conditions for the Schrödinger Equation*, Riv. Mat. Univ. Parma **6** (2001), 57–108.

[15] T. Hagstrom, *Radiation boundary conditions for the numerical simulation of waves*, Acta Numerica **8** (1999), 47–106.

[16] H. Han and Z. Huang, *Exact Artificial Boundary Conditions for the Schrödinger Equation in* $\mathbb{R}^2$, Comm. Math. Sci. **2** (2004), 79–94.

[17] W. Huang, C. Xu, S.-T. Chu and S.K. Chaudhuri, *The finite–difference vector beam propagation method: Analysis and assessment* J. Lightwave Technology **10** (1992), 295–304.

[18] M.F. Levy, *Non–local boundary conditions for radiowave propagation*, in: Third International Conference on Mathematical and Numerical Aspects of Wave Propagation Phenomena, Juan-les-Pins, France, 24-28 April 1995.

[19] M.F. Levy, *Parabolic equation models for electromagnetic wave propagation*, (IEE Electromagnetic Waves Series 45, 2000).

[20] C. Lubich and A. Schädle, *Fast convolution for non–reflecting boundary conditions*, SIAM J. Sci. Comput. **24** (2002), 161–182.

[21] B. Mayfield, *Non–local boundary conditions for the Schrödinger equation*, Ph.D. thesis, University of Rhode Island, Providence, RI, 1989.

[22] A. Schädle, *Numerische Behandlung transparenter Randbedingungen für die Schrödinger–Gleichung*, Masters Thesis, Universität Tübingen, 1998.

[23] A. Schädle, *Non–reflecting boundary conditions for the two dimensional Schrödinger equation*, Wave Motion **35** (2002), 181–188.

[24] F. Schmidt and P. Deuflhard, *Discrete transparent boundary conditions for the numerical solution of Fresnel's equation*, Comput. Math. Appl. **29** (1995), 53–76.

[25] F. Schmidt, *Construction of discrete transparent boundary conditions for Schrödinger–type equations*, Surv. Math. Ind. **9** (1999), 87–100.

[26] I.L. Sofronov, *Conditions for Complete Transparency on the Sphere for the Three–Dimensional Wave Equation*, Russian Acad. Sci. Dokl. Math. **46** (1993), 397–401.

[27] I.L. Sofronov, *Artificial Boundary Conditions of Absolute Transparency for Two- and Threedimensional External Time–Dependent Scattering Problems*, Euro. J. Appl. Math. **9** (1998), 561–588.

[28] I.L. Sofronov, *Non–reflecting inflow and outflow in wind tunnel for transonic time–accurate simulation*, J. Math. Anal. Appl. **221** (1998), 92–115.

[29] F.D. Tappert, *The parabolic approximation method*, in *Wave Propagation and Underwater Acoustics*, Lecture Notes in Physics 70, eds. J.B. Keller and J.S. Papadakis, Springer, New York, 1977, pp. 224–287.

[30] A. Zisowsky, *Discrete Transparent Boundary Conditions for Systems of Evolution Equations*, Ph.D. Thesis, Technische Universität Berlin, 2003.